

Itinerant-3*d*-electron spin-density oscillations surrounding solute atoms in Fe

Mary Beth Stearns

Scientific Research Staff, Ford Motor Company, Dearborn, Michigan 48121

(Received 8 August 1974)

A previous method of analysis of hyperfine-field spectra of dilute Fe-based alloys with transition solute atoms to the right of Fe in the periodic table is extended to obtain the solute- and host-moment perturbations of dilute Fe-based alloys with any 3*d* or 4*d* transition element. The resulting host-moment perturbations show very simple oscillatory behavior which can be interpreted as due to spin density oscillations in the itinerant *d* electrons. It is shown that these spin density oscillations can be thought of as arising from the polarization induced in the itinerant *d* electrons by the localized *d* moment via mainly Coulomb exchange interactions, whereas the localized moments arise from the intra-atomic exchange interaction between the localized *d* electrons. Within this scheme a purely itinerant band ferromagnetism is not plausible. The value of the Curie temperature of Fe is shown to be in good agreement with the interpretation. The features that are important in determining alloy behavior are clearly seen in this analysis and are enumerated and discussed. The contrast in behavior with dilute Ni-based alloys is also briefly discussed.

I. INTRODUCTION

For the past decade there has been much activity in measuring and interpreting the solute-moment and host-moment perturbations which arise when transition-metal elements are substitutionally dissolved in Fe or Ni. Most of the information thus far has come from average-saturation-magnetization and neutron diffuse-elastic-scattering experiments.^{1,2} The saturation-magnetization data provide information only about the total change in moment, whereas the neutron scattering data give information about the individual moment distributions. However the neutron scattering data are obtained in wave-vector space so they must be Fourier transformed to obtain the spatial moment distributions. These are difficult experiments and the region of *k* space measured is small so the resulting solute moments and host perturbation are determined only roughly.

Recently we have developed a method which uses hyperfine-field (hff) data to give much more detailed information about the solute-moment and the host-moment perturbations.³ This paper will be referred to as I. This method has previously been used to evaluate the solute moments and host-moment perturbations developed in dilute alloys of Fe with transition elements to the right of Fe in the periodic table (Co, Ni, and Rh). In these cases the host-moment perturbations are positive and fall off nearly as $1/r^3$. Here we extend a variation of the method to elements below and to the left of Fe (Mn, Cr, V, Ru, and Mo). This analysis is given in Secs. II and III. The model⁴ of the 3*d* transition metals underlying this analysis is that at the beginning of the transition series all the *d* electrons are itinerant. Then

as the nuclear charge increases across the series, the electrons tend to become more tightly bound. At some point some of the *d* electrons become localized due to the increased binding and the atoms then develop a moment. However a few of the *d* electrons (e.g., ~5% in Fe) remain itinerant. These itinerant *d_i* electrons are polarized through Coulomb exchange and hybridization interactions with the localized *d* electrons. This provides the Ruderman-Kittel-Kasuya-Yosida (RKKY)-like polarization⁵ which aligns the localized *d_i* electrons, either ferromagnetically or antiferromagnetically depending on the number of *d_i* electrons. This model will be further discussed in Section IV. We shall see that it becomes obvious from the present results that a natural way to interpret the host-moment perturbations are as being due to the spin density oscillations of the itinerant *d_i* electrons. Previously some of the moment perturbations have been explained in terms of virtual *d* levels^{6,7} and charge screening effects.⁸ However these types of explanations have been unsuccessful in explaining many details of the data,² and whereas this concept may be important in dilute alloys of transition metals in nonmagnetic hosts, we do not believe it plays a dominant role in the alloys considered here.

In this analysis of mainly average saturation magnetization, hyperfine field and neutron scattering data of dilute alloys with Fe as host, three features emerge as principally determining the behavior of electrons in alloys: (i) The electrons of each atom in an alloy strongly tend to preserve their elemental environment, i.e., they compromise their behavior somewhat toward the other constituents but tend to remain as in their pure state. (ii) Although the itinerant electrons can

easily pass between adjacent atomic cells, when in a cell of an atom with valence electrons of the same orbital symmetry they strongly take on the atomiclike character of those electrons when in that cell. This feature has been applied extensively in explaining the value of the hff at nontransition solute atoms in Fe,^{4,9} specifically in the assumption that the 4s-conduction-electron contribution scales as the atomic hff coupling constant. (iii) The degree of hybridization of the various types of electrons of each of the atomic constituents in their elemental environment is very important. It is a measure of the ease with which these electrons can take on the different orbital characters of the atoms, either within an atomic cell or for itinerant electrons as they pass from atomic cell to atomic cell.

The evolution of theories of disordered alloy systems incorporate the above features in increasing degrees of sophistication. The most simplistic approach is the rigid-band approximation which describes feature (i) by assuming that, in binary alloys, the density of states of both transition-metal elemental constituents are similar. Such a simple approach, of course, cannot describe anything but average values; such quantities as host-moment perturbations are entirely beyond its spirit. The coherent-potential method^{10,11} incorporates feature (i) by using an effective Hamiltonian to describe an effective medium for the alloy and feature (ii) by using tight-binding wave functions to represent the valence electrons for the two types of atoms in the alloys. The earlier theories were single-band models and thus could not describe feature (iii). More recent extensions¹² take into account more complex band models which allow hybridization to be represented in the theories. Reference 11 discusses and gives a comparison of many other disordered-binary-alloy theories.

In Sec. IV we show that the well-known RKKY-type derivations⁵ of the form of the spin-density oscillations for the 4s conduction electrons are equally valid for the itinerant *d* electrons at distances of greater than about one-half a lattice spacing. In Sec. V we give the interpretation of the observed host-moment perturbations in Fe. In Sec. VI we briefly discuss the behavior of dilute Ni alloys.

In the following paper¹³ (called III) we Fourier transform the moment distributions obtained from the hff spectra to obtain curves to compare with the neutron data on dilute Fe alloys. All the features of the neutron data are reproduced very well. However, we often obtain solute-moment values in Fe which are quite different from those obtained in Ref. 1. In III we show that this is be-

cause under some conditions the assumptions made in the neutron data analysis to determine the solute moments are not valid.

II. DESCRIPTION OF HYPERFINE-FIELD ANALYSIS

In all cases considered here the solute atoms are small, so there are no volume overlap contributions to the hyperfine field.^{4,9} Furthermore, since the orbital moment is quenched in Fe, the hff comes predominantly from the *s* electrons. The hff produced at an Fe nucleus can thus be considered as arising from sum of the polarizations p_{ns} of the *s* electrons for each shell coupled through the hff coupling constants H_{ns}^{fc} , i.e., $H_{Fe} = \sum p_{ns} H_{ns}^{fc}$. At this time we do not know all these individual terms but, fortunately for the present purposes, we only need to know certain partial combinations of this sum which can be determined experimentally. Thus for pure Fe we break the hff up into contributions of the core *s* electrons (1s, 2s, 3s), H_{cp} , and the 4s-conduction-electron polarization (sCEP) contribution. It is convenient to further consider the sCEP term as the sum of two terms: the first the polarization of the 4s electrons by an atom itself H_s ; the second the sum of the sCEP due to the surrounding Fe atoms H_Σ . H_Σ is known for an Fe lattice since the contributions to sCEP for each shell surrounding an Fe atom, ΔH_n^{fc} , have been deduced from measurement in FeSi and FeAl alloys,^{9,14} where the Si and Al atoms develop no moment and give rise to negligible host moment perturbations.¹⁵ These sCEP contributions ΔH_n^{fc} , for the various shells surrounding an Fe atom, are listed in Table I as set A. We thus have

$$H_{Fe} = H_{cp} + H_s + H_\Sigma, \quad (1)$$

where $H_\Sigma = \sum_n M_n \Delta H_n^{fc} \mu_{Fe}^e (= -145 \text{ kG})$ and M_n is the number of Fe atoms in the *n*th shell. H_Σ can also be independently obtained from the hff of small nonmagnetic solute atoms dissolved in Fe. This is further discussed in Ref. 4 where we found that H_Σ was between -140 and -170 kG from the hff's at Cu, Ag, and Au nuclei in Fe. Since $H_{Fe} = -346 \text{ kG}$, the hff contribution from an Fe atom itself is thus $H_M = H_{cp} + H_s = -201 \text{ kG}$ or $-90.5 \text{ kG}/\mu_B$. As long as only the Fe spectra of dilute alloys is considered we need only this fairly well-known sum H_M for this analysis. It is the hff produced at an Fe atom due to its own moment. There is a possibility that the signs of the third (*N3*) and sixth (*N6*) nearest-neighbor shifts might be negative instead of positive as given in set A. This would be so if the hff at Si in Fe and Fe₃Si were positive instead of negative as assumed in Ref. 9. It has not been determined. To see what

TABLE I. Values of quantities used in the evaluation of the hyperfine field shifts of an Fe atom near a solute atom.

Shell		N1	N2	N3	N4	N5	N6
M_n		8	6	12	24	8	6
ΔH_n^{hc} (kG/ μ_B)	Set A ^a	-12.1	-2.7	+2.4	+0.6	+0.3	+0.6
	Set B ^b	-11.0	-0.9	-2.4	+2.0	+1.1	-0.6
				$H_\Sigma = -145$ kG			
				$H_\Sigma = -150$ kG			

^a These values are those obtained in Ref. 9.

^b This is a reasonable set with N3 and N6 taken as negative.

effect this would have on this analysis we have made up a reasonable set of hff shifts for pure Fe where N3 and N6 are negative and $H_\Sigma = -150$ kG. These are listed as set B in Table I.

The philosophy of the general procedure of analyzing the Fe hff spectra of these dilute alloys with transition element solute atoms is the following. Whereas ideal nontransition solute atoms, like Al and Si, act like magnetic holes in the Fe lattice and thus cause the sCEP contributions from the missing Fe atoms to be absent, the transition element solute atoms have two effects: (i) if they develop a moment, they contribute a sCEP contribution from their own moment; and (ii) they cause moment perturbations on the nearby Fe atoms which change the H_{cp} , H_s , and H_Σ contributions from these Fe atoms. We take all these effects into account.

In analyzing the Fe spectra of dilute alloys, we make the reasonable assumption that the probability of the 4s electrons being in each atomic cell throughout the alloy is the same as that in pure Fe. We further assume that the spatial form of the sCEP surrounding any moment is the same as that in pure Fe and that its magnitude is proportional to the moment. In the case where we are considering the sCEP coming from a moment on the solute atom, this implicitly assumes the solute-moment spin-density distribution is similar to that of the Fe moment.⁴ Neutron form-factor measurements in general give spin distributions which are atomiclike and are very similar for the 3d transition series,¹⁶ thus indicating that this is a reasonable assumption for the 3d series. The atomiclike 4d wave functions have two maxima, one closer in and one further out than the 3d maxima. The measured neutron form factor of paramagnetic Pd (Ref. 17) indicates that the moment density may be about 20% more expanded than that of Fe. The sCEP magnitude due to such a moment would be expected to be about 20% smaller per μ_B than that from Fe.⁴ However, we are concerned with the sCEP oscillation *difference* between the missing Fe moment and the moment

on the 4d solute atom. At most the 4d-series solute atom moments are about $1\mu_B$ so the sCEP for the worst cases might be weakened by about 10% compared to that for pure Fe. In the cases where the solute moment is small (e.g., Mo), the magnitude of the sCEP is essentially that due to the missing Fe moment, so no error is made. Thus taking the sCEP to have the same shape as in pure Fe and scaling as the moment should also be a reasonable procedure for the 4d transition series. Furthermore, since some of the moment comes from the itinerant d electrons this assumption implies, as we shall discuss further in Sec. IV, that when the itinerant d electrons are in an atomic cell that possesses a local d moment, they strongly take on the atomiclike d-spin-density distribution typical of the atom in that cell. If the itinerant d's are in an atomic cell which has no moment, they are expected to have very little polarization and a rather uniform spatial probability distribution function. The results of the neutron scattering experiments in dilute alloys¹ had also already shown that the moment distributions are atomiclike since any uniform polarization would give a scattering distribution which would predominately occur at scattering vector Q near zero. This polarization would have been missed in the neutron experiments since the lowest Q values measured were $\sim 0.3\text{\AA}^{-1}$. However, the measured neutron scattering cross sections when extrapolated into $Q=0$ agreed well with the average moment change per solute atom, $d\bar{u}/dc$, as measured in average saturation magnetization experiments, thus indicating that there is little polarization with a nonatomiclike distribution.

When a transition element solute atom goes substitutionally into an Fe lattice, it may develop a moment and also perturb the moments on the nearby Fe atoms. Since here the hff measures only the polarization of s electrons at the nucleus, it detects changes in the distribution of d electrons only through the interaction of the s electrons with the atomiclike moments of the d electrons. Letting

the Fe moment perturbations be represented by Δ_n , where n is the n th shell surrounding the solute atom, we can write down the hff shift ΔH_n^z for Fe atoms in each shell surrounding the solute atom Z . This was done in I. There we listed in Table II the occupational distribution for the Fe atoms in the first four neighbor shells to the solute atom. We then kept track of all the sCEP contributions from each of the surrounding atoms,

$$\begin{aligned}
 \Delta H_1^z &= H_M \Delta_1 + \Delta H_1^{\text{Fe}} (\mu_Z - \mu_{\text{Fe}} + 3\Delta_2 + 3\Delta_3 + \Delta_5) + \Delta H_2^{\text{Fe}} (3\Delta_1 + 3\Delta_4) + \Delta H_3^{\text{Fe}} (3\Delta_1 + 6\Delta_4) \\
 &\quad + \Delta H_4^{\text{Fe}} (3\Delta_2 + 6\Delta_3 + 3\Delta_5 + 3\Delta_6), \\
 \Delta H_2^z &= H_M \Delta_2 + \Delta H_1^{\text{Fe}} (4\Delta_1 + 4\Delta_4) + \Delta H_2^{\text{Fe}} (\mu_Z - \mu_{\text{Fe}} + 4\Delta_3 + \Delta_6) + \Delta H_3^{\text{Fe}} (4\Delta_2 + 4\Delta_5) + \Delta H_4^{\text{Fe}} (4\Delta_1 + 8\Delta_4), \\
 \Delta H_3^z &= H_M \Delta_3 + \Delta H_1^{\text{Fe}} (2\Delta_1 + 4\Delta_4) + \Delta H_2^{\text{Fe}} (2\Delta_2 + 2\Delta_5) + \Delta H_3^{\text{Fe}} (\mu_Z - \mu_{\text{Fe}} + 4\Delta_3 + 2\Delta_6) + \Delta H_4^{\text{Fe}} (4\Delta_1 + 6\Delta_4), \\
 \Delta H_4^z &= H_M \Delta_4 + \Delta H_1^{\text{Fe}} (\Delta_2 + 2\Delta_3 + \Delta_5 + \Delta_6) + \Delta H_2^{\text{Fe}} (\Delta_1 + 2\Delta_4) \\
 &\quad + \Delta H_3^{\text{Fe}} (2\Delta_1 + 3\Delta_4) + \Delta H_4^{\text{Fe}} (\mu_Z - \mu_{\text{Fe}} + 2\Delta_2 + 3\Delta_3 + 2\Delta_5).
 \end{aligned} \tag{2}$$

Summing the coefficients of the Δ_n 's for the $\Delta H_{\text{Fe}}^{zn}$ values in set A we get

$$\begin{aligned}
 \Delta H_1^z &= -12.1(\mu_Z - \mu_{\text{Fe}}) - 91.4\Delta_1 - 34.5\Delta_2 - 32.7\Delta_3 \\
 &\quad + 6.3\Delta_4 - 10.3\Delta_5 + 1.8\Delta_6, \\
 \Delta H_2^z &= -2.7(\mu_Z - \mu_{\text{Fe}}) - 46\Delta_1 - 80.9\Delta_2 - 10.8\Delta_3 \\
 &\quad - 43.6\Delta_4 + 9.6\Delta_5 - 2.7\Delta_6, \\
 \Delta H_3^z &= 2.4(\mu_Z - \mu_{\text{Fe}}) - 21.8\Delta_1 - 5.4\Delta_2 - 80.9\Delta_3 \\
 &\quad - 44.8\Delta_4 - 5.4\Delta_5 + 4.8\Delta_6, \\
 \Delta H_4^z &= 0.6(\mu_Z - \mu_{\text{Fe}}) + 2.1\Delta_1 - 10.9\Delta_2 - 22.4\Delta_3 \\
 &\quad - 88.7\Delta_4 - 10.9\Delta_5 - 12.1\Delta_6.
 \end{aligned} \tag{2a}$$

including the solute atom. Combining this with the polarization produced by the Fe atom itself we derived formulas for the hff shifts for Fe atoms in the first four neighbor shells surrounding a solute atom whose moment is μ_Z . Considering the first four sCEP terms and moment perturbations in the first six shells surrounding the solute atom, the general formulas are

It can be seen from the above formulas that the main contributions to the hff shifts ΔH_n^z come from H_M and ΔH_1^{Fe} since these are by far the larger terms.

From the behavior of the average saturation magnetization we also have another equation relating μ_Z and the Δ_n values. It is the equivalent of Eq. (2) of I and is given by

$$\frac{d\bar{\mu}}{dc} = \mu_Z - \mu_{\text{Fe}} + \sum_{n=1}^6 M_n \Delta_n, \tag{3}$$

where $d\bar{\mu}/dc$ is the initial slope of the variation of average moment $\bar{\mu}$ with concentration c of the

TABLE II. Hyperfine fields and derived moments at nd -transition series elements in Fe.

z	Solute	H_Z^{Fe} (kG) ^a	H_{cp}^z (kG/ μ_B) ^b	H_{ns}^z (MG)	μ_Z (μ_B)	Neut. ^d μ_Z (μ_B)
23	V	-94	-156	1.4	-0.2 ± 0.1	-0.4 ± 0.4
24	Cr	-52 (calc) -110 (calc)	-163	1.6	-0.7 (assumed) 0.0 (assumed)	-0.7 ± 0.4
25	Mn	(-) 234	-168	1.8	1.0 ± 0.2	0 ± 0.2
26	Fe	-346	-172	2.0	2.22	
27	Co	-295	-177	2.2	1.9 ± 0.1 ^c	2.1 ± 0.5
28	Ni	(-) 241	-181	2.4	1.4 ± 0.1 ^c	0.9 ± 0.15
$H_s^{\text{Fe}} = 81 \text{ kG}/\mu_B$						
42	Mo	-263		3.3	0.2 ± 0.2	-0.1 ± 0.6
44	Ru	-505		4.0	1.0 ± 0.2	0.9 ± 0.5
45	Rh	-557		4.4	1.1 ± 0.2 ^c	0.5 ± 0.3
46	Pd	-537		4.8	1.0 ± 0.2 ^c	0.1 ± 0.2
$H_{\text{cp}}^{4d} \sim -370 \text{ kG}/\mu_B$						

^a $\frac{4}{3}\pi M_s = 7 \text{ kG}$ has been subtracted from the measured values.

^b Variation as calculated in Ref. 19.

^c Obtained in Ref. 3.

^d Obtained in Ref. 1.

solute atom, i.e., $\bar{\mu} = \mu_{\text{Fe}} + c d\bar{\mu}/dc$. It has been measured for all cases considered here. For elements to the right of Fe, the neutron experiments had indicated that the Δ_n 's were all positive and that they decreased with distance from the solute atom.¹ In I we therefore assumed a functional form for the Δ_n values which fell off as the m th power of the distance from the solute atom; the ΔH_n^Z 's then became only a function of two parameters μ_Z and Δ_1 . For these alloys the Fe hff spectra have extra structure that is spread over a small range on the high-frequency side of the pure Fe line. The ΔH_n^Z 's are small (typically ~ -5 kG) and overlap greatly. However the shape of the spectra is very sensitive to μ_Z and Δ_1 so by fitting the Fe spectra of these alloys we could ascertain values for Δ_1 and μ_Z . We found that a $1/r^3$ behavior of the Δ_n 's gave by far the best fit. We will see that we can understand this behavior since the spin-density oscillations due to a Coulomb exchange interaction in the region before the first node vary roughly as $1/r^3$.^{4,9} The μ_Z values obtained in this way agreed well with those deduced from the hff value measured at the solute atom.

For the elements below and to the left of Fe, the Fe spectra are well spread out; the ΔH_1 and ΔH_2 values are large (typically $\sim +20-30$ kG) and thus are obtained directly from the Fe spectra. ΔH_3 is quite a bit smaller but in some cases was also obtained from the Fe spectra. For these elements we used the measured value of the hff at the solute atom to determine μ_Z in the following way. In I we also derived the expression for the hff H_Z at a solute atom entirely surrounded by Fe atoms. It is given by the properly modified sum of the core polarization and conduction-electron contributions [see discussions leading to Eq. (15) of I]

$$H_Z^{\text{in Fe}} = \left(H_{\text{cp}}^{\text{nd}} + \frac{H_{\text{ns}}^Z H_s^{\text{Fe}}}{H_{4s}^{\text{Fe}}} \right) \mu_Z + \frac{H_{\text{ns}}^Z}{H_{4s}^{\text{Fe}}} \sum_{n=1}^6 M_n \Delta H_n^{\text{Fe}} (\mu_{\text{Fe}} + \Delta_n). \quad (4)$$

The H_Z values were obtained from the measured values by subtracting the Lorentz term $\frac{4}{3} \pi M_s$ ($=7$ kG) from the measured hff to obtain the true hff. These are listed in column 3 of Table II. $H_{\text{cp}}^{\text{nd}}$ is the contribution per μ_B to the hff from core polarization in the nd transition series. H_{ns}^Z is the hyperfine coupling constant of atom Z ; these are listed in column 5 of Table II. H_s^{Fe} is the self-polarization per μ_B of the 4s conduction electrons by the Fe atom. For the 3d series solute atoms, the atomiclike spin distributions are considered to be close enough to that of an Fe atom that the

same value of H_s^{Fe} is used as that obtained for pure Fe. For the 4d series we make the same assumption, this implies that the radial spin distribution of the 4d series is similar to that of Fe, as discussed earlier.

As discussed in I, there is some doubt as to what the values of $H_{\text{cp}}^{\text{Fe}}$ and H_s^{Fe} are individually; however their sum is known very well from experiment. Band-theory calculations^{4,18} of $H_{\text{cp}}^{\text{Fe}}$ yield a value of -380 kG or -172 kG/ μ_{Fe} , which gives $H_s^{\text{Fe}} = 180$ kG or 81 kG/ μ_B . However an analysis of only hff data in I indicated that $H_{\text{cp}}^{\text{Fe}}$ might possibly be as much as -315 kG/ μ_B and $H_s^{\text{Fe}} = +224.5$ kG/ μ_B . Fortunately since mainly the difference of these two quantities enters [except for the factor $H_{\text{ns}}^Z/H_s^{\text{Fe}}$ in front of H_s^{Fe} , Eq. (4)] both sets of values lead to the same values of μ_Z to within $0.1 \mu_B$. Here we use the band calculation values to obtain the moments. For the 3d series, the H_{cp} values are believed to increase by about 15% from V to Ni^{19,20}; these values are listed in column 4 of Table II. However these small variations lead to a difference of less than $0.1 \mu_B$ from the values obtained by assuming H_{cp}^Z is constant and equal to $H_{\text{cp}}^{\text{Fe}}$ across the series. The H_{cp}^{d} value appears to be quite constant across the 4d series.²¹ In I we found $H_{\text{cp}}^{\text{Rh}} + H_s^{\text{Rh in Fe}} = -190$ kG/ μ_B , taking $H_s^{\text{Rh in Fe}} = H_{5s}^{\text{Rh}}/H_{4s}^{\text{Fe}} \times 81 = 178$ kG/ μ_B we get $H_{\text{cp}}^{\text{Rh}} \simeq -370$ kG/ μ_B . This is the same as the calculated value²¹ and we use it for H_{cp}^{d} here.

We used an iterative procedure to evaluate the μ_Z 's. Since the Δ_n values always turn out to be small compared to μ_{Fe} , as a first approximation we ignore the Δ_n 's in Eq. (4). We then used the derived value of μ_Z to obtain the Δ_n values as discussed below. We then put these Δ_n 's back into Eq. (4) and repeated the procedure. The corrected value of μ_Z was always within $0.1 \mu_B$ of the first value. The final values obtained for μ_Z are listed in column 6 of Table II. The values of μ_Z obtained from the hff are sometimes not in very good agreement with those obtained in the neutron scattering experiments which are listed in column 7 of Table II. As we shall discuss in III, some of the approximations made to determine the moments in the neutron work were often not valid and therefore in some cases these values could be quite wrong.

The procedure used to obtain the Δ_n values was as follows: since we know ΔH_1 , ΔH_2 (and sometimes ΔH_3), μ_Z , and $d\bar{\mu}/dc$, we have three (or four) independent equations relating the Δ_n 's. Since the Δ_n values decrease rapidly at large distances and the fourth and fifth shells are very close in radii (also the 1st and 2nd, see Fig. 1) we can in general obtain values for combinations

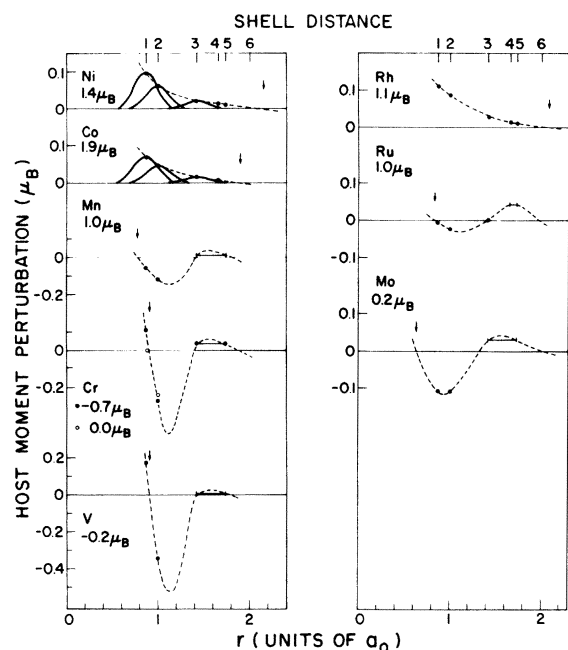


FIG. 1. Host-moment perturbations surrounding transition-metal solute atoms as a function of distance from the solute atom. Note that the ordinate scale factor for Mn, Cr, and V is a factor of 2 larger than for the other elements.

of the first five Δ_n 's. This is now discussed in more detail under each solute atom.

III. EXPERIMENTAL RESULTS

Ni and Co

The μ_z and Δ_n values for these have been determined and discussed in I. They are listed in Table III. The Δ_n values are shown plotted in Fig. 1. We have shown these values connected by a dashed curve. This is just for convenience; in actuality there is a $3d$ atomiclike spin density situated around each lattice site as indicated by the bell shaped curve shown by the solid lines in

the graphs for Co and Ni. Again these bell shaped curves are only pictorial, they should be shaped like $3d$ radial distribution function with zero value at the origin. We see in the following paper that the Fourier transforms of the solute-moment and host-moment perturbations agree excellently with the neutron scattering results.

Mn

The Mn hff spectra have been measured many times by both Mössbauer^{14,22,23} and NMR techniques.^{24,25} As discussed in I the Mössbauer technique has inherently poorer resolution than properly carried out NMR experiments. The experiments of the author in Ref. 14 were carefully computer analyzed considering four or five neighbor shells for many different concentrations. In Ref. 22, Wertheim *et al.* carried out their analysis in terms of first- and second-neighbor shifts and a multiplicative concentration-dependent factor. This probably leads to somewhat inaccurate values in some cases, especially for ΔH_2 . Vincze and Campbell²³ have made an investigation of all the d transition elements in Fe but use the same type of analysis as in Ref. 22. They used a least-squares analysis to obtain the best fit, and their results seem about the same as those of Ref. 22. The NMR measurements have much better inherent resolution, but much of the data for these alloys were taken before the complexities of this technique were fully appreciated.^{9,26} Thus the spectra of Ref. 24 seem to show too little intensity in the satellites, a type of inaccuracy common to the early spin echo experiments as was discussed in I. We list shifts for FeMn alloys in Table IV. All the data given here is adjusted to correspond to 0°K. Since the hff values are negative, the signs of the ΔH_n given here correspond to the actual sign of the shift caused by the solute atom, i.e., positive ΔH_n decreases the resonance frequency of a given spectrum component. For that

TABLE III. Derived solute moments μ_z and host-moment perturbations Δ_n (in μ_B) of the n th shell surrounding the solute atom.

Solute	μ_z	Δ_1	Δ_2	Δ_3	Δ_4	Δ_5
Ni	1.4 ± 0.1	0.095	0.062	0.022	0.013	0.012
Co	1.9 ± 0.1	0.07	0.045	0.016	0.01	
Mn	1.0 ± 0.2	-0.06	-0.11		← 0.016 →	
Cr	-0.7	0.11	-0.28		← 0.03 →	
	0.0	0.0	-0.24		← 0.03 →	
V	-0.2 ± 0.1	0.17	-0.35		← 0.01 →	
Rh	1.1 ± 0.2	0.11	0.075	0.026	0.016	0.014
Ru	1.0 ± 0.2	-0.0076	-0.023	0.002	← 0.043 →	
Mo	0.2 ± 0.2	-0.11	-0.11		← 0.03 →	

TABLE IV. Hyperfine field shifts ΔH_n (in kG) for Fe Mn.

	ΔH_1	ΔH_2	ΔH_3
ME ^a	25	15	-8
ME ^b	23	4	

^a Reference 14. ME, Mössbauer effect.

^b Reference 22.

reason (a decrease in frequency) the ΔH_n are often listed in the literature with the opposite sign to that used here. We observed in Ref. 14 that ΔH_2 decreased rapidly with Mn concentration; thus the low value for ΔH_2 in Ref. 22 may be due to this effect (the concentration was not listed). Since we want the shifts for the most dilute alloy we use the values close to those of Ref. 14, $\Delta H_1 = 24$ kG and $\Delta H_2 = 15$ kG. The value of $d\bar{\mu}/dc$ is $-2.11 \mu_B$, almost simple dilution.²⁷ The value obtained for the moment of Mn was about $1.0 \pm 0.2 \mu_B$. Besides being obtained from the hff at the Mn atom this value is also in agreement with that obtained by analyzing the temperature dependence of the hff at the Mn atom and its nearest-neighbor Fe atoms.²⁸ As is well known this value does not agree with that obtained in Ref. 1, $\mu_{Mn} \sim 0\mu_B$, however other neutron scattering experiments²⁹ have shown that Mn does have a moment. This will be discussed further in III. So in this case we have three simultaneous equations involving the Δ_n 's and solved for Δ_1 , Δ_2 , and let $\Delta_3 = \Delta_4 = \Delta_5$. We also tried many other combinations (e.g., $\Delta_1 = \Delta_2$, Δ_3 , $\Delta_4 = \Delta_5$) but the above procedure seemed to be the best since the oscillations are expected to decrease rapidly with distance from the solute atom. All reasonable groupings gave rise to oscillations with negative values required for at least one of the first three nearest neighbors. This type of behavior of a definite negative oscillation was not sensitive to the value of ΔH_2 varying from 0 to 15 kG. Thus the general moment perturbation behavior is definitely different from that of Co and Ni and has a distinctive negative oscillation in the region of the first few neighbors. The Δ_n values obtained for set A are listed in Table III and shown plotted in Fig. 1. The Δ_n values obtained for set B were very similar to those obtained for set A. In general we found Δ_1 was slightly more negative and Δ_2 slightly more positive than those of set A, while the sum of $\Delta_1 + \Delta_2$ was about the same for both sets. The Δ_3 through Δ_5 and μ_z value were essentially unchanged.

Cr

The number of atoms in the N1 and N2 shells are very close, 8 and 6, respectively. Thus it is

difficult when ΔH_1 and ΔH_2 are nearly the same to be sure in any analysis of only the spectra which shift goes with which shell. Cranshaw *et al.*^{30,31} have used these alloys to measure the dipolar shifts resulting from a solute atom. They used the Mössbauer technique and measured the difference spectra of single crystals of FeCr with a magnetic field applied in the $\langle 100 \rangle$ and $\langle 111 \rangle$ directions. The dipolar broadening for the N1 and N2 shells is different for the different magnetization directions and they gave the assignment of the larger shift as being due to the N1 shell. Since this type of measurement should be sensitive to this feature, we use their assignment. We list the various values of ΔH_n from different experiments in Table V. We use $\Delta H_1 = 34$ kG and $\Delta H_2 = 24$ kG in the analysis here. The slope of the saturation magnetization curve is $d\bar{\mu}/dc = -2.29$.²⁷ We thus again have three simultaneous equations relating the Δ_n 's and μ_{Cr} . Unfortunately the hff value at the Cr atom in Fe has not been measured. The shape of the neutron scattering curve in these alloys strongly indicates that the value of μ_{Cr} is negative and around $-0.7\mu_B$. Assuming this value, we solve for Δ_1 , Δ_2 , and $\Delta_3 = \Delta_4 = \Delta_5$. The resulting hff at Cr is ~ -52 kG which should occur at about 11 MHz. This solution for set A is shown in Fig. 1 and listed in Table III. These values give excellent agreement with the neutron scattering curve for FeCr alloys. We also calculated the Δ_n 's assuming $\mu_{Cr} \approx 0.0\mu_B$. These are listed for set A in Table III and plotted in Fig. 1 as the open circles. This leads to a hff at Cr of $H_{Cr} \sim -110$ kG which would give a resonance at ~ 25 MHz. This solution gives fair agreement with the neutron scattering data so a determination of the hff at Cr is needed to determine the Cr moment more accurately. The value of the Δ_n 's found in analyzing the neutron experiments³² seem to be unlikely, since they lead to pairs of shifts for ΔH_1 and ΔH_2 of either 49 and 11 kG, or 45 and 20 kG for the $\Delta_1 = \Delta_2$ solution. Both of these sets are incompatible with the measured values of $\Delta H_1 = 34$ kG and $\Delta H_2 = 24$ kG. As we shall see in Sec. V a negative value of

TABLE V. Hyperfine field shifts ΔH_n (in kG) for FeCr.

	ΔH_1	ΔH_2	ΔH_3
ME ^a (2.0%)	29	32.5	9
ME ^b	28	24	
ME ^c (4.8%)	34.5	24 ^d	

^a Reference 14.

^b Reference 22.

^c References 30 and 31.

^d Called ΔH_5 in Refs. 30 and 31.

the Cr moment would follow naturally from the antiferromagnetic coupling resulting from introducing a large number of itinerant d 's in the vicinity of the Cr solute atom.

There has long been a controversial interpretation of the Mössbauer data by Cranshaw.³¹ He argued that since ΔH_2 for $FeSi$ was close to zero, ΔH_2 for $FeCr$ could not be as large as 24 kG and therefore this shift should be assigned to ΔH_5 . Furthermore, since the N1 and N5 atoms are in the same direction $\langle 111 \rangle$, he concluded that the sCEP was very anisotropic. We see here that the host-moment perturbations can easily make ΔH_2 large and thus his arguments are invalid.

V

The measured hff shifts for V are listed in Table VI. As usual all these values are extrapolated to 0 K. The agreement of all the data is quite good. A more recent spin-echo experiment³³ also found $\Delta H_1 \simeq \Delta H_2$. So we use $\Delta H_1 = 25$ kG and $\Delta H_2 = 26$ kG. The value of $d\bar{\mu}/dc = -2.69$.²⁷ From the measured value of the V hff we obtain from Eq. (4) that $\mu_V = -0.2 \pm 0.1 \mu_B$. This agrees with the value obtained from neutron scattering experiment¹ $\mu_V = (-0.4 \pm 0.4) \mu_B$. We thus have three simultaneous equations connecting the Δ_n 's and again solve for Δ_1 , Δ_2 , and $\Delta_3 = \Delta_4 = \Delta_5$. The resulting Δ_n values for set A are given in Table III and shown plotted in Fig. 1.

Pd

A solution for Pd which used Fallot's³⁴ measured $d\bar{\mu}/dc = -0.2 \mu_B$ was given in I. This solution gave $\mu_{Pd} = (0.7 \pm 0.2) \mu_B$ with Δ_n 's decreasing roughly as $1/r^3$ and $\Delta_1 = 0.066 \mu_B$. However the neutron data¹ look as if $d\bar{\mu}/dc \simeq 1 \mu_B$. The measured value of $d\bar{\mu}/dc$ is very questionable since only (1-2)% of Pd is soluble in the bcc phase of Fe.³⁵ The lowest dilution Fallot measured was 3.4% thus it is likely that his alloys had segregated regions of fcc Fe. Since the fcc regions would have no moment, this

TABLE VI. Hyperfine field shifts ΔH_n (in kG) for FeV.

	ΔH_1	ΔH_2	ΔH_3
ME ^a (2.2%)	25	26	-5
ME ^b (4-16%)	26	22	
ME ^c	← 25 →		
SE ^d	← ~24 →		

^a Reference 14.

^b Reference 22.

^c Reference 23.

^d Reference 33. SE, spin echo.

may be the reason he obtained a negative slope. All the other transition elements to the right of Fe have a positive $d\bar{\mu}/dc$ varying from $0.8 \mu_B$ to $1.9 \mu_B$. Thus it is likely that the slope for Pd in the soluble region is also positive; however since it is unknown we present no data for Pd. The ΔH_n values obtained in I are thus likely to be incorrect for Pd. This would also result in the value of the core polarization for the $4d$ transition series being different from the value given in I. We thus use the value derived from only Rh, i.e., H_{cp}^{4d} in Fe = -370 kG/ μ_B . This agrees with the calculated value of -370 kG/ μ_B and would yield a value of $\mu_{Pd} \simeq (1.0 \pm 0.2) \mu_B$.

Rh

From the Fe hff and $d\bar{\mu}/dc = 1.1 \mu_B$ for Rh alloys, the moment of Rh was found to be $(1.1 \pm 0.2) \mu_B$ and $\Delta_1 = 0.11 \mu_B$ for a $1/r^3$ decrease of the Δ_n values. These are listed for set A in Table III and shown plotted in Fig. 1.

Ru

The $FeRu$ shifts have been determined quite accurately from spin-echo experiments by Murphy *et. al.*³⁶ They obtained $\Delta H_1 = 16$ kG, $\Delta H_2 = 4$ kG, and $\Delta H_3 = -5$ kG to about 1 kG. The value of $d\bar{\mu}/dc$ is zero.³⁴ We determine that $\mu_{Ru} = 1.0 \pm 0.1$ from the hff at Ru using $H_{cp}^{4d} = -370$ kG/ μ_B and $H_s^{4d} = 81H_{5s}^{Fe}/H_{4s}^{Fe}$ kG/ μ_B . We thus have four simultaneous equations relating the Δ_n 's and solve for Δ_1 , Δ_2 , Δ_3 , and $\Delta_4 = \Delta_5$. The Δ_n values are listed for set A in Table III and shown in Fig. 1. The Δ_n values are all quite small and therefore are very sensitive to the exact values of the hff shifts. Thus it would be very advantageous to know these shifts even more accurately.

Mo

The $FeMo$ hff shifts are rather well known since a 3.2 at. % Mo single crystal was studied extensively³⁷ in a Mossbauer-type experiment to obtain the anisotropic dipolar interactions. The shifts obtained were $\Delta H_1 = 37$ kG and $\Delta H_2 = 18$ kG. We determine $\mu_{Mo} = (0.1 \pm 0.2) \mu_B$ from the hff at the Mo nucleus. The value of $d\bar{\mu}/dc = -2.2 \mu_B$, essentially simple dilution.³⁸ We thus have three simultaneous equations relating the Δ_n 's. Solving these for Δ_1 , Δ_2 , and $\Delta_3 = \Delta_4 = \Delta_5$ we get the values listed for set A in Table III and shown plotted in Fig. 1.

Clearly better data for all the alloys to the left of Fe would be very desirable. Most of the data for these alloys should be improvable by using presently attainable optimum resolution conditions in spin-echo experiments.^{9,26} We found that the Δ_n

values are mainly sensitive to the H_M and ΔH_1^{Fe} values and thus set A and set B give only slightly different values for Δ_1 and Δ_2 with their sum, μ_z and $\Delta_3 - \Delta_5$ being about the same for both sets. Thus the Fourier transform of both sets are essentially indistinguishable and we use only set A in Paper III.

IV. DISCUSSION OF ASSUMPTIONS MADE IN ANALYSIS

A. Characteristics of d electrons

The author has proposed⁴ that the ferromagnetism in Fe, Co, and Ni arises from the indirect coupling, via Coulomb exchange and interband mixing interactions, of mainly localized (>95%) d electrons (d_l) by a small number ($\leq 5\%$) of itinerant d electrons (d_i). Some of the characteristics of itinerant d electrons in Fe have become clear from considerations of various experiments and calculations. Band-structure calculations³⁹ for Fe indicate that there are pure d_l bands which are parabolic with $E_{d_l} \approx \hbar^2 k^2 / 2m_e^*$, where $m_e^* = 2m_e$. Furthermore m_e^* is essentially the same for the d_l 's as for the 4s conduction electrons, see Fig. 2 of Ref. 4. de Haas-van Alphen measurements⁴⁰ show that these d_l 's have a nearly spherical Fermi surface just as do s conduction electrons in free-electronlike metals. Since the d_l 's are more confined in k space than the d_i 's the uncertainty principle indicates that they are more spread out in r space than the d_i 's and thus they have some probability of being in different atomic cells. This behavior is in contrast to that of the localized portion of the wave function describing the d_l electrons. For the d_l electrons the bands are quite flat, i.e., high or infinite effective mass, they have no Fermi surface and negligible probability of being outside their atomic cell. Thus it appears that the itinerancy of the d electrons is similar to that of the 4s conduction electrons; the main difference being that each has a different orbital symmetry.

In considering the detailed mechanism of the coupling of the d_l electrons by the d_i electrons, we shall neglect their hybridization and treat the d_l polarization as if it only arises from the Coulomb exchange interaction. We expect, from the form of the sCEP curve, the hybridization is present, but whereas the hybridization does affect the details of the sCEP curve, the general behavior should be adequately obtained from considering only the Coulomb exchange interaction. We will show that it is reasonable that the spin-density oscillations of the d_l electrons (d SDO, this is interchangeable with the term d CEP), at distances greater than $\frac{1}{2}$ lattice spacing, can be represented by a polarization curve similar to that for Coulomb

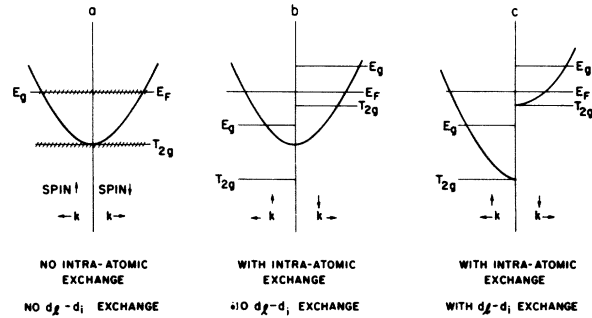


FIG. 2. Schematic representation of the interactions which give rise to the ferromagnetism of Fe. The flat bands represent the localized d electrons; the parabolic band, the itinerant d electrons.

exchange between localized d electrons and itinerant s electrons; i.e., the RKKY⁵ interaction.

Let us first consider how the d_l electrons obtain their polarization. The schematic representation of the behavior of the d electrons is shown in Fig. 2. The flat bands represent the d_l electrons and the parabolic bands the d_i electrons. In Fig. 2(a) we envision a simplified d -band structure for a hypothetical paramagnetic Fe (not Fe above the Curie temperature) which has no intra-atomic Coulomb exchange interactions (i.e., no Hund's rule) and no Coulomb exchange interactions between the d_l and d_i electrons. In this case the Fermi level falls somewhere inside the E_g bands, as indicated, since there are about seven d electrons/atom with about 0.3 electron/atom being itinerant. In Fig. 2(b) we have turned on only the intra-atomic exchange interaction, which splits the localized spin-up and spin-down E_g and T_{2g} states as shown by an amount ΔE . This gives rise to a local moment. A point worth noting is that the intra-atomic exchange interaction has no effect on the itinerant d_i electrons (Cr, V, Ti, and Sc all have only itinerant d 's and develop no moments; we are not concerned here with ground-state spin-density waves⁴¹ in the conduction electrons, as in Cr and neglect them). The itinerant electrons are not on a given atom long enough for intra-atomic exchange to be effective.

The question of when a localized moment occurs has been one which has received much attention for the case of magnetic ions in nonmagnetic hosts.^{6,7} For the case of ferromagnets we see that almost by definition the condition for formation of a local moment is; the moment becomes localized when the band width Γ of a given d state is less than the intra-atomic exchange interaction. We say "almost by definition" since in the band picture, flat bands mean large Δk for small energy widths; according to the uncertainty principle

these electrons then have a small enough Δr to be considered localized. Thus in ferromagnetic materials, the ferromagnetism itself is a built-in criteria to indicate that the bands have become flat enough compared with the intra-atomic exchange energy to produce localization. Under this condition some of the d electrons are on a given atom long enough so that the intra-atomic exchange interaction can be effective and produce a moment. Since $S=1$ for Fe, we have about two unpaired electrons and the intra-atomic exchange energy U is $\sim \frac{1}{2}\Delta E$. The localization condition is thus $\Gamma \sim U$, where Γ here refers to the half-width of a single localized electron state. This condition is often stated in terms of the density of states, since $\Gamma_d \sim 1/n_d(E)$.

It should be pointed out that we never expect the width Γ to get much smaller than the intra-atomic exchange interaction energy for the $3d$ transition series. This occurs because, in this case where we have the ferromagnetism arising from interactions of d_i and d_j electrons, we expect that both the hybridization and intra-atomic exchange interactions are of comparable magnitude; since they both arise from Coulomb interactions between electrons of the same orbital character. Thus the width Γ due to hybridization is given by $\Gamma \sim \pi U^2 \rho_{d_i}$.⁷ In order that Γ be smaller than U we need $U < 1/\pi \rho_{d_i}$. Since the effective mass of the d_i electron in Fe is about $2m_e$, ρ_{d_i} is about $\frac{1}{6} \text{eV}^{-1}$ and thus $\Gamma < U$ when $U < 2 \text{eV}$. However for the $3d$ transition $U \sim 1.5 \text{eV}$,⁴² so the half widths of the localized levels are expected to be comparable to the spin splitting. It is a well observed fact that experimental density of states for the $3d$ transition series⁴³ never show the narrow density-of-states structure obtained by band calculations.³⁹ The above considerations suggest that part of the reason for this is that the band calculations do not contain enough hybridization to broaden the states realistically.

For a given transition series, the intra-atomic exchange energy per electron is about constant. Thus at some point across a series the binding of the d states may become large enough, due to the increase in Z , so that the widths of some of the d states become comparable to the intra-atomic exchange energy. For the first transition series, this is only the condition for formation of a local moment; it is a necessary but not sufficient condition to obtain ferromagnetism. For that we need a few d_i electrons to provide communication between the localized d_i 's. Going back to Fig. 2, in (b) we have turned on the intra-atomic exchange but still have no d_i - d_j exchange interaction and therefore the d_i 's are unpolarized. In (c), we also turn on the d_i - d_j exchange interaction. This pro-

duces the polarization in the d_i 's. Notice that this explanation of ferromagnetism makes purely itinerant band ferromagnetism implausible for two reasons: (i) the intra-atomic exchange interaction does not act on itinerant electrons, and (ii) within this scheme too many itinerant d electrons would be unlikely to lead to a ferromagnetic coupling. Thus we envision that Fe has mainly d_i electrons which are polarized due to intra-atomic Coulomb exchange and a few d_j electrons which are polarized by the d_i - d_j Coulomb exchange interaction. We can show that one can directly apply the usual RKKY-type calculations for unpolarized s conduction electrons to the d_i 's. As we shall see, the only difference will be that the u_k 's in Bloch-type wave functions $\varphi_k(r) = u_k(r)e^{i\vec{k}\cdot\vec{r}}$ have d -like orbital character instead of s -like character. Since the wave functions of the itinerant electrons are very atomiclike close to the nucleus, the main portion of the polarization of the d_i 's occurs within the atomic d_i radius, with a relatively small tail reaching into the interstitial region and beyond. This small fraction of polarization, however, aligns the local moments. The hff and neutron scattering experiments are not accurate enough to measure (or miss) the small amount of polarization in the outer reaches of the atomic cells. In a sense the hff data, as treated, have some incorporation of this extended distribution, since the measured ΔH_n^{Fe} values of Table I correspond to the true moment distribution in Fe and thus reflect the fact that some of moment comes from the polarization of the d_i 's with large spatial extent.

Since the polarization of the d_i 's is very atomiclike in spatial distribution, the argument used in Ref. 44 to estimate the fraction of itinerant d_i 's is invalid. The expression for the average hff of purely itinerant d electrons given in Ref. 44 as Eq. (22) assumed that the polarization of the d_i 's was uniformly distributed throughout the alloy. To terms linear in concentration c , the present picture of polarization would always lead to the average hff falling off about as $(1 - cH_E/H_{Fe})$, as observed. Since there is ample other evidence for a small fraction of d_i 's, this estimate is not crucial.

B. Details of d_i -electrons spin-density oscillations due to d_i - d_j Coulomb exchange interaction

In RKKY theory the exchange integral is given by^{5,45}

$$J(\vec{k}, \vec{k}') = \int \int \varphi_{\vec{k}}^*(\vec{r}_1) \psi_d(\vec{r}_1) \frac{1}{r_{12}} \psi_d^*(\vec{r}_2) \times \varphi_{\vec{k}'}(\vec{r}_2) d\tau_1 d\tau_2, \quad (5)$$

where φ_k and $\varphi_{k'}$ are the conduction-electron orbitals and ψ_d the local moment orbitals. The resulting spin-density oscillations are given by

$$\rho_{\pm}(\vec{r}) = \mp S \sum_{\vec{k}=0}^{k_F} \sum_{\vec{k}'=0}^{\infty} \frac{J(\vec{k}, \vec{k}')}{\epsilon_{\vec{k}} - \epsilon_{\vec{k}'}} [\varphi_{\vec{k}}^*(\vec{r}) \varphi_{\vec{k}'}(\vec{r}) + \varphi_{\vec{k}}(\vec{r}) \varphi_{\vec{k}'}^*(\vec{r})], \quad (6)$$

where S is the local moment spin. The usual approximations made in evaluating the SDO's are:

(i) $\varphi_k = V^{-1/2} e^{i\vec{k}\cdot\vec{r}}$, i.e., u_k is taken as a constant, (ii) $J(\vec{k}, \vec{k}')$ is a function only of $\vec{Q} = \vec{k} - \vec{k}'$, and (iii) $\epsilon_k = \hbar^2 k^2 / 2m$. With these approximations Eq. (6) becomes simply

$$\rho(r)_{\pm} = \mp S \int \chi(Q) J(Q) (e^{i\vec{Q}\cdot\vec{r}} + e^{-i\vec{Q}\cdot\vec{r}}) dQ, \quad (7)$$

where $\chi(Q)$ is the noninteracting free electron spin susceptibility given by

$$\chi(Q) = \chi_P \left(\frac{1}{2} + \frac{1-x^2}{4x} \ln \left| \frac{1+x}{1-x} \right| \right), \quad (8)$$

where χ_P is the Pauli susceptibility and $x = Q/2k_F$. This simplified version of RKKY theory applies equally well to *s* or *d_i* conduction electrons, and identical results would be obtained for *d_i-s* or *d_i-d_i* exchange interactions. Various investigations have been made of the approximations made in Eq. (7). Kaplan⁴⁶ investigated the effect of not assuming $u_k = \text{const}$, independent of k . He used single plane waves orthogonalized to the core electrons (OPW) to represent the *s* conduction electrons in the factor $[\varphi_{\vec{k}}^*(\vec{r}) \varphi_{\vec{k}'}(\vec{r}) - \varphi_{\vec{k}}(\vec{r}) \varphi_{\vec{k}'}^*(\vec{r})]$ in Eq. (6). He found that for distances $> \frac{1}{2}a$, where a is the lattice constant, the results are essentially identical for $u_k = \text{const}$ and for OPW's. In a similar manner the u_k values for OPW's of the *d_i* conduction electrons are also expected to only affect $\rho(r)$ at distances in close to the atomic core and thus the *d_i* conduction electrons have a similar SDO behavior to that of the *s* conduction electrons for $r > \frac{1}{2}a$. Kaplan also reasoned that a similar behavior applied to $J(\vec{k}, \vec{k}')$ in Eq. (6). The effects of the second approximation were examined by Watson and Freeman.⁴⁵ They used OPW's in evaluating $J(\vec{k}, \vec{k}')$ but only plane waves for the φ_k term in Eq. (6). They found that the approximation of using $J(Q)$ was often not very good, with the main differences occurring at small r . Their type treatment could equally well be extended to OPW's that represent *d_i* instead of *s* conduction electrons.

C. Behavior near Curie temperature

An interesting question is whether the behavior of Fe is as expected near the Curie temperature

T_c ? Band calculations³⁹ as well as comparison of experimental data⁴² indicate, from the splitting of the E_g^{\uparrow} and E_g^{\downarrow} levels in Fe, that the intra-atomic exchange spin splitting is about 3 eV. Thus the intra-atomic exchange energy U for Fe is about 1.5 eV. Since T_c for Fe corresponds to an interaction energy of $kT_c \approx 0.1$ eV available to unalign the spins, clearly we expect essentially the same band structure above T_c as below it. Thus there should be no appreciable change in the moment or density of states in going through T_c . That the moment doesn't change appreciably is well known from two experiments: (i) susceptibility measurements⁴⁷ above T_c which show μ_{Fe} to be nearly the same above as below T_c and (ii) analysis⁴⁸ of specific-heat measurements which show that in Fe the entropy increase in going through T_c is about $Nk \ln 3$, thus indicating that $S=1$ above T_c . That the band structure or density of states does not change is seen from: (i) photoelectron-energy distribution curves⁴⁹ for Ni which show no change above and below T_c , and (ii) neutron scattering experiments⁵⁰ of the spin-wave spectrum of Ni and Fe which show very little change in the spin-wave character above and below T_c . Any changes in band structure through T_c would be expected to be even more evident in Ni than in Fe, so we conclude that there are no observable changes in the band structure of Fe in going through T_c . Since the moment alignment is believed to be due to the *d*CEP, let us see if the information we have gives a reasonable alignment energy for this mechanism. Owing to the atomiclike spacial behavior of the *d_i*'s, the *d_i-d_i* Coulomb exchange and intra-atomic exchange interactions should be of similar strength. Thus we expect the *d*CEP caused by a given Fe moment to be "locked into" that local moment with an interaction energy comparable to the intra-atomic interaction energy, $U \sim 1.5$ eV. Each local moment is then aligned by the sum of the *d*CEP contributions from the surrounding Fe atoms. The condition for the spins obtaining local moment disorder is when the thermal energy becomes comparable to the energy of alignment, i.e., when

$$kT_c \approx U \vec{S} \cdot \sum_n \Delta \vec{s}_n, \quad (9)$$

where Δs_n is the *d_i* contribution of spin polarization from an Fe atom in the *n*th shell, and we have summed over the *d_i* spin contributions of all the surrounding Fe atoms. Since $S \approx 1$ for Fe, we find from Eq. (9) that $\sum_n \Delta s_n \approx 0.05-0.1$ or $\sum_n \Delta \rho_n = 0.1-0.2 \mu_B$. Since $\Delta \rho_n(r)$ varies roughly as $1/r_n^3$ in the region before the first node, summing over such a variation for the first three neighbor shells (we assume the higher shells can be neglected since

their $\Delta\rho_n$'s are small and tend to cancel due to oscillations) gives $\sum_n \Delta\rho_n \approx 15\Delta\rho_1$; thus $\Delta\rho_1 \approx 0.01\mu_B$. Band-structure calculations and de Haas-van Alphen measurements have shown that there are about 0.3 (d_i electrons)/atom which are highly polarized. Thus, we find a self-polarization of about $0.1\mu_B$ caused by the Fe atom itself. This gives a ratio for the d_i spin density on an atom to the value at $N1$, $\Delta\rho_0/\Delta\rho_1$ of about 10–30. This is a reasonable value for a d CEP curve of the RKKY type. Thus we find that the values of T_c , U , and the number of d_i 's are all consistent with the idea that the Fe spins are mainly localized and coupled through d CEP.

V. INTERPRETATION OF RESULTS

The outstanding features of the host moment perturbations found in Sec. III are that they are oscillatory in form (for elements to the right of Fe the negative portion of the oscillation is far out and thus has a small amplitude) with the first nodes moving in a systematic way. The first nodes are marked by arrows in Fig. 1. We show that these features follow naturally if the host moment perturbations are caused by the itinerant d_i electrons. The $1/r^3$ falloff of the host moment perturbations for transition elements to the right of Fe fits in this picture very naturally since the form of a spin-density oscillation in the region before the first node varies roughly as $1/r^3$.^{4,9} The SDO's surrounding a local moment are well known to have an oscillatory form which falls off rapidly with distance and oscillates roughly as a function of $2k_F r$,⁵ even at intermediate r .⁴⁵ If some interband mixing is present the same general behavior occurs; i.e., the oscillations are still a function of $2k_F r$ and fall off rapidly with distance but details of the shape are different⁵¹ and the polarization is more negative at small distances. In any case the first node occurs around $2k_F r \approx \text{const}$.

At the beginning of any d transition series the d electrons are all itinerant and the d bands and s band have about the same width. In crossing the series the d -band widths become narrower due to the increased binding as the nuclear charge increases. For the $3d$ series this is manifest by the fraction of d electrons which are itinerant decreasing as we cross the series. We know that all the d electrons are itinerant through Cr.⁴¹ Then at Mn some of the bands have become narrow enough that the intra-atomic exchange interaction dominates and Mn develops a local moment.⁵² However in this case a large number of d 's are still itinerant so that the Fermi wave vector k_F for these d_i 's is large and the first node for Mn falls inside the nearest-neighbor ($N1$) distance.

This is similar to the situation for the d_i - s interaction in Fe,^{4,9} and leads to Mn being antiferromagnetic. However for Fe, Co, and Ni most of the d electrons have become localized with less than about 5% being itinerant. Thus the k_F values for these d_i 's are small and the first node of the d CEP falls beyond the $N1$ distance. This gives rise to the ferromagnetism in these elements.

In dilute alloys of one transition element in another, the number of d_i electrons is appreciably perturbed in the vicinity of the solute atom. This then changes the shape of the polarization curve of the d_i electrons, via the d_i - d_i exchange interaction, in the vicinity of the solute atom. The nearby Fe atoms sense this directly as a change in their moments since the excess (or deficit) d_i electrons take on a strong atomiclike character when in the atomic cells of the nearby Fe atoms. Although the host moment perturbations are made up of contributions from all the nearby atoms and are thus very complex in detail, when substituting a solute atom to the right (left) of Fe we expect a deficit (excess) number of d_i electrons relative to pure Fe, and since a smaller (larger) number of d_i electrons corresponds to d CEP curves whose first nodes occur at larger (smaller) distances we expect the first nodes of the d CEP curves of elements to the right (left) of Fe to move farther out (closer in) than that in pure Fe. This is just the behavior seen in the host moment perturbations in Fig. 1 for both the $3d$ and $4d$ series. We also might expect that some of the solute atoms to the left of Fe might become antiferromagnetically coupled in the Fe lattice when the excess number of itinerant d 's is large enough to cause the d CEP first node at the solute atom to move inside the distance to the solute atom. We see that indeed this happens for both Cr and V. In Table VII, we list the solute moments μ_Z , the measured $d\bar{\mu}/dc$, and the total host-moment perturbations $\Delta\mu_h$, as obtained here from the hff data and average-saturation-magnetization data. We see that there appears to be definite systematic behavior of μ_Z and $d\bar{\mu}/dc$ in these alloys. This naturally results from the systematic behavior of the d_i 's and d_i 's in crossing a transition series. The $\Delta\mu_h$ values thus also reflect this systematic behavior. However, we would like to emphasize that the $\Delta\mu_h$ values do *not* represent the excess or deficit number of d_i 's introduced into the lattice by the solute atom. As in the case of the hff contributions of the s CEP, it represents a lattice weighted average of the form of the polarization of the perturbed host lattice. For Ni and Co solute atoms, there are a deficit number of d_i 's but we see that the net polarization $\Delta\mu_h$ increases because the d CEP curve has a larger spatial extent. For Mn and V

TABLE VII. Solute moments and host moment perturbations in dilute Fe alloys.

Solute	$\mu_z(\mu_B)$	$d\bar{\mu}/dc(\mu_B)$	$\Delta\mu_h(\mu_B)$
Ni	1.4	1.00	1.8
Co	1.9	1.04	1.3
Mn	1.0	-2.11	-0.9
Cr	0.0 to -0.7	-2.29	-0.1 to 0.6
V	-0.2	-2.69	-0.3
Rh	1.1	1.1	2.2
Ru	1.0	0	1.2
Mo	0.2	-2.2	-0.2

the excess number of d_i 's introduced into the lattice causes a net decrease in the host magnetization due to the negative portion of the d CEP curve moving in closer and thus becoming more prominent. For Cr an appreciable negative Cr moment would introduce some d CEP of opposing sign and thus could reverse the sign of $\Delta\mu_h$ from that of Mn and V solute atoms.

VI. COMMENTS ON BEHAVIOR OF Ni ALLOYS

It is conspicuous that in the past^{7b,53} Ni has usually been cited as exhibiting the prototype behavior of a completely itinerant ferromagnet whereas here we propose that it has mainly localized d electrons. The previous interpretation arose for a number of reasons, mostly connected with the small moment and the fact that some of the localized spin-down states are straddling the Fermi level.⁵⁴ Since the moment of Ni is smaller than that of Fe, a greater fraction of the moment is due to d_i 's with the result that in some measurements their influence *appears* to be more important in Ni than in Fe.

Dilute Ni- and Fe-based alloys show strikingly different average saturation magnetization and neutron elastic-diffuse-scattering behavior. Whereas many Fe alloys with nontransition solute atoms show simple dilution and very little host-moment perturbations; the analogous Ni alloys show average moment decreases of an amount per solute atom which are about equal to the difference in the number of outer valence electrons of the solute atom⁵⁵ and the number of 4s electrons on the displaced Ni atom, and large host-moment perturbations on the nearby Ni atoms.⁵⁶ In the past, this decrease in average moment per solute atom has often been interpreted as indicating that the outer valence electrons were going into the d bands of Ni and filling up the holes in the spin-down bands.^{7b} Such simple reasoning is, however, inconsistent with the fact that the electron screening requires that each atomic cell be essentially neu-

tral and therefore the valence electrons of the solute atom are not available to fill the Ni d bands. Furthermore, evidence that the d bands are not filled when the moment disappears in NiCu alloys comes from low-temperature specific-heat measurements⁵⁷ which show that there is a much greater density of states than expected from just s electrons and thus there are still d states at the Fermi level when the ferromagnetic state disappears. All of the above results can be understood by considering that the behavior of these Ni alloys is mainly due to the hybridization of the s , d_i , and d_i electrons of Ni combined with the location of the unfilled localized states of Ni. Using the formulas developed by Moriya⁵⁸ we have shown in Ref. 59 that the average saturation magnetization data can be understood as resulting from the hybridization interactions of the s , d_i , and d_i electrons causing the moments to decrease on the Ni atoms in the vicinity of the solute atom. Since the localized states of Fe are far from the Fermi level there are little or no moment perturbations on Fe atoms in the vicinity of the solute atom and thus Fe shows only simple dilution. On the other hand Co has an even greater density of states of d_i spin-down electrons near the Fermi level than Ni, so we expect that the moment decrease per solute atom in Co alloys may be greater than in Ni alloys. This appears to be so for Al and Si solute atoms.⁶⁰

Since the host moment perturbations cause large hff core polarization contributions, we expect the Ni hff spectra for the Ni-based alloys to be very different from the analogous Fe hff spectra. As yet very few Ni hff spectra have been measured,⁶¹ but it would be of great interest to have these for a series of alloys, e.g., especially Cu, Zn, Al, Si, Co, and Fe, to compare with the magnetization and neutron scattering measurements. That the Ni spectra are indeed appreciably different from the Fe spectra is seen in Ref. 61 where spectra of Al, V, Cr, and Co alloys are reported. An attempt to interpret these spectra using two terms, one an average local moment and the other an average alloy moment was made in Ref. 61. However only general prominent features were discussed and no attempt was made to calculate the detailed spectra shapes. These data were also taken before the complexities of ferromagnetic NMR were understood,^{9,26} and thus the angle of turn of the nuclei was not held constant across the spectra. As we discussed in I, this can lead to incorrect intensities in the satellites. It is of special interest that Co and Fe solute atoms in Ni should play a similar role to Al and Si in Fe-based alloys. This arises because the solute hff, magnetization, and neutron scattering measurements all indicate that there is little if any host moment

perturbations when Co or Fe are alloyed with Ni. Thus the sCEP for Ni should be directly obtainable from CoNi or FeNi alloys.

VII. CONCLUSIONS

A method has been developed to obtain the solute- and host-moment perturbations from hyperfine field spectra of dilute Fe-based alloys with 3d and 4d transition elements. The resulting host moment perturbations show very simple oscillatory behavior which can be interpreted as due to the change in number and thus polarization of itinerant d electrons in the vicinity of the solute

atom. The justification is given for treating these spin-density oscillations as arising from the polarization induced in the itinerant d electrons by the localized d_i moment via Coulomb exchange and interband interactions. It is shown that the Curie temperature of Fe is in good agreement with this interpretation. In the following paper (III) the spatial behavior of the solute- and host-moment perturbations is Fourier transformed into momentum space and is seen to give results in good agreement with the measured neutron diffuse-elastic-scattering cross sections of these alloys.

- ¹M. F. Collins and G. G. Low, Proc. Phys. Soc. Lond. **86**, 535 (1965).
- ²J. B. Comly, T. M. Holden, and G. G. Low, J. Phys. C **1**, 458 (1968).
- ³M. B. Stearns, Phys. Rev. B **9**, 2311 (1974), hereafter referred to as I. The data analyzed in this paper were those of J. I. Budnick, T. J. Burch, S. Skalski, and K. Raj, Phys. Rev. Lett. **24**, 511 (1970).
- ⁴M. B. Stearns, Phys. Rev. B **8**, 4383 (1973).
- ⁵M. A. Ruderman and C. Kittel, Phys. Rev. **96**, 99 (1954); T. Kasuya, Prog. Theor. Phys. **16**, 45 (1956); K. Yosida, Phys. Rev. **106**, 893 (1957), hereafter referred to as RKKY.
- ⁶J. Friedel, Nuovo Cimento Suppl. **2**, 287 (1958); J. Friedel, G. Leman, and S. Olszewski, J. Appl. Phys. Suppl. **32**, 325 (1961).
- ⁷(a) P. W. Anderson, Phys. Rev. **124**, 41 (1961); P. A. Wolff, *ibid.* **124**, 1030 (1961). (b) For a discussion of much of this work see N. F. Mott, Adv. Phys. **13**, 325 (1964).
- ⁸J. Kanamori, J. Appl. Phys. **36**, 929 (1965); H. Hayakawa, Prog. Theor. Phys. **37**, 213 (1967); I. A. Campbell and A. A. Gomes, Proc. Phys. Soc. Lond. **91**, 319 (1967).
- ⁹M. B. Stearns, Phys. Rev. B **4**, 4069 (1971); **4**, 4081 (1971).
- ¹⁰P. Soven, Phys. Rev. **156**, 809 (1967); **178**, 1136 (1969).
- ¹¹B. Velicky, S. Kirkpatrick, and H. Ehrenreich, Phys. Rev. **175**, 747 (1968).
- ¹²S. Kirkpatrick, B. Velicky, and H. Ehrenreich, Phys. Rev. B **1**, 3250 (1970); K. Levin and H. Ehrenreich, *ibid.* **3**, 4172 (1971); P. N. Sen, *ibid.* **8**, 5613 (1973).
- ¹³M. B. Stearns and L. A. Feldkamp, following paper, Phys. Rev. B **13**, 1198 (1976), referred to as III.
- ¹⁴M. B. Stearns and S. S. Wilson, Phys. Rev. Lett. **13**, 313 (1964); M. B. Stearns, Phys. Rev. **147**, 439 (1966).
- ¹⁵A. Arrott, M. F. Collins, T. M. Holden, G. G. Low, and R. Nathans, J. Appl. Phys. Suppl. **37**, 1194 (1966); T. M. Holden, J. B. Comly, and G. G. Low, Proc. Phys. Soc. Lond. **92**, 726 (1967).
- ¹⁶C. G. Shull and Y. Yamada, J. Phys. Soc. Jpn. Suppl. **17**, 1 (1962); C. G. Shull, in *Electronic Structure and Alloy Chemistry of the Transition Elements*, edited by P. A. Beck (Interscience, New York, 1963), p. 69;
- R. M. Moon, Phys. Rev. **136**, A195 (1964); H. A. Mook, *ibid.* **148**, 495 (1966); R. M. Moon, Int. J. Magn. **1**, 129 (1971).
- ¹⁷J. W. Cable, Bull. Am. Phys. Soc. **19**, 355 (1974); and private communication.
- ¹⁸The latest band calculation of Duff gives $H_{cp} = -380$ kG (private communication). Since this is in agreement with the various calculated values discussed in Ref. 3 we will use this value.
- ¹⁹R. E. Watson and A. J. Freeman, Phys. Rev. **123**, 2027 (1961).
- ²⁰R. Winkler, Phys. Lett. **23**, 301 (1966).
- ²¹A. J. Freeman, B. Bagus, and R. E. Watson, Colloq. Int. Cent. Natl. Rech. Sci. **164**, (1966); R. E. Watson and A. J. Freeman, *Hyperfine Interactions* (Academic, New York, 1967), p. 53.
- ²²G. K. Wertheim, V. Jaccarino, J. H. Wernick, and D. N. E. Buchanan, Phys. Rev. Lett. **12**, 24 (1964). Analyzed for only two neighbor shells and a concentration-dependent multiplicative factor.
- ²³I. Vincze and I. A. Campbell, J. Phys. F **3**, 647 (1973).
- ²⁴M. Rubinstein, G. H. Stauss, and M. B. Stearns, J. Appl. Phys. **37**, 1334 (1966).
- ²⁵M. Rubinstein, G. H. Stauss, and J. Dweck, Phys. Rev. Lett. **17**, 1001 (1966).
- ²⁶M. B. Stearns, Phys. Rev. **162**, 496 (1967); M. B. Stearns and J. F. Ullrich, Phys. Rev. B **4**, 3825 (1971).
- ²⁷A. Arrott and J. E. Noakes, *Iron and Its Dilute Alloy* (Wiley, New York, 1963), p. 23.
- ²⁸G. G. Low, Phys. Lett. **21**, 497 (1966); D. A. Shirley, S. S. Rosenbaum, and E. Matthais, Phys. Rev. **170**, 363 (1968); M. B. Stearns (unpublished).
- ²⁹N. Kroo, L. Pal, and D. Jovic, in *Fourth IAEA Symposium on Neutron Inelastic Scattering* (IAEA, Vienna, 1968), Vol. II, p. 37.
- ³⁰T. E. Cranshaw, C. E. Johnson, M. S. Ridout, and G. A. Murray, Phys. Lett. **21**, 481 (1966).
- ³¹T. E. Cranshaw, J. Phys. F **2**, 615 (1972).
- ³²M. F. Collins and G. G. Low, J. Phys. (Paris) **25**, 596 (1964).
- ³³R. H. Dean, R. J. Furley, and R. G. Scurlock, J. Phys. F **1**, 78 (1971).
- ³⁴M. Fallot, Ann. Phys. **10**, 291 (1938).
- ³⁵M. Hansen, *Constitution of Binary Alloys* (McGraw-Hill, New York, 1958).

- ³⁶J. J. Murphy, T. J. Burch, and J. I. Budnick, AIP Conf. Proc. 10, 1627 (1972).
- ³⁷A. Asano and L. H. Schwartz, AIP Conf. Proc. 18, 262 (1973).
- ³⁸S. Arajs, Phys. Status Solidi 31, 217 (1969).
- ³⁹S. Wakoh and J. Yamashita, J. Phys. Soc. Jpn. 21, 1712 (1966); K. J. Duff and T. P. Das, Phys. Rev. B 3, 192 and 2294 (1971); R. A. Tawil and J. Callaway, *ibid.* 7, 4242 (1973).
- ⁴⁰A. V. Gold, L. Hodges, P. T. Panousis, and D. R. Stone, Int. J. Magn. 2, 357 (1971).
- ⁴¹A. W. Overhauser, Phys. Rev. 128, 1437 (1962).
- ⁴²The location of the $E_{\frac{1}{2}}^{\uparrow}$ level with respect to the $3p_{3/2}$ level can be obtained rather well from the soft-x-ray emission spectra of D. H. Tomboulian and D. E. Bedo [Phys. Rev. 121, 146 (1961)]. The location of the $E_{\frac{1}{2}}^{\uparrow}$ level with respect to $3p_{3/2}$ is well located in x-ray absorption measurements of B. Sonntag, R. Haensel, and C. Kunz [Solid State Commun. 7, 597 (1969)] or electron scattering experiments of M. B. Stearns and L. A. Feldkamp, AIP Conf. Proc. (to be published). Thus ΔE can be obtained.
- ⁴³See, for example, the soft-x-ray spectra in Ref. 41 and *Electronic Density of States*, edited by L. H. Bennett, Natl. Bur. Stds. Special Publication No. 323 (U.S. GPO, Washington, D. C., 1971).
- ⁴⁴M. B. Stearns, Phys. Rev. B 6, 3326 (1972).
- ⁴⁵R. E. Watson and A. J. Freeman, Phys. Rev. 152, 566 (1966); 178, 725 (1969).
- ⁴⁶T. A. Kaplan, Phys. Rev. Lett. 14, 499 (1965).
- ⁴⁷W. Sucksmith and R. R. Pearce, Proc. R. Soc. A 167, 189 (1938).
- ⁴⁸J. A. Hofman, A. Paskin, K. J. Taner, and R. J. Weiss, J. Phys. Chem. Solids 1, 45 (1956).
- ⁴⁹D. T. Pierce and W. E. Spicer, Phys. Rev. B 6, 1787 (1972).
- ⁵⁰H. A. Mook, J. W. Lynn, and R. M. Nichlow, Phys. Rev. Lett. 30, 556 (1973); J. W. Lynn, *ibid.* B 11, 2624 (1975).
- ⁵¹R. E. Watson, S. Koide, M. Peter, and A. J. Freeman, Phys. Rev. 139, A167 (1965); R. E. Watson, A. J. Freeman, and S. Koide, Phys. Rev. 186, 625 (1969).
- ⁵²This is confirmed strikingly by the shape of the $3p \rightarrow 3d$ core transitions. That for Cr has the usual shape seen in normal metals, i.e., a Fermi edge with extended structure indicating no local moments. However, Mn through Ni have the very different dispersive shape due to interference between a localized state and continuum states (see Ref. 42).
- ⁵³See, e.g., C. Herring, in *Magnetism*, edited by G. T. Rado and H. Suhl (Academic, New York, 1966), Vol. IV.
- ⁵⁴S. Wakoh, J. Phys. Soc. Jpn. 20, 1894 (1965); L. Hodges, H. Ehrenreich and N. D. Lang, Phys. Rev. 152, 505 (1966); J. Callaway and H. M. Zhang, Phys. Rev. B 1, 305 (1970); E. I. Zornberg, *ibid.* 1, 244 (1970); J. Langlinais and J. Callaway, *ibid.* 5, 124 (1972).
- ⁵⁵J. Crangle and M. J. C. Martin, Philos. Mag. 4, 1006 (1959); J. Crangle, in *Electronic Structure and Alloy Chemistry of the Transition Elements*, edited by P. A. Beck (Interscience, New York, 1963).
- ⁵⁶J. B. Comly, T. M. Holden, and G. G. Low, J. Phys. C 1, 458 (1968).
- ⁵⁷W. H. Keesom and B. Kurrelmeyer, Physica 7, 1003 (1940); G. L. Guthrie, S. A. Friedberg, and J. E. Goldman, Phys. Rev. 113, 45 (1959); K. P. Gupta, C. H. Cheng, and P. A. Beck, *ibid.* 133, A203 (1964).
- ⁵⁸T. Moriya, Prog. Theor. Phys. 33, 157 (1965).
- ⁵⁹M. B. Stearns, AIP Conf. Proc. 24, 453 (1975).
- ⁶⁰D. Parsons, W. Sucksmith, and J. E. Thompson, Philos. Mag. 3, 1174 (1958).
- ⁶¹R. L. Streever and G. A. Urriano, Phys. Rev. 139, A135 (1965); 149, 295 (1966).